JET PRODUCTION IN *ep* COLLISIONS

PIERRE VAN MECHELEN [a]
Universiteit Antwerpen

Results obtained by the H1 and ZEUS Collaborations on jet production in photoproduction and deep-inelastic scattering are presented and compared to NLO QCD models.

1 Introduction

The observation of jet production at HERA allows to test the theory of strong interactions, quantum chromodynamics (QCD), and to extract information on the parton content of the proton and of real or virtual photons. QCD predicts the production of partons with large transverse momenta, fragmenting into jets with similar four-momenta. The study of jet observables therefore allows to investigate the underlying parton dynamics. Perturbative QCD predictions, however, also need the parton content of the proton and photon as input. Jet cross sections can thus be used to further constrain the parton density functions (PDF's) obtained by global fits.

The clustering of final state objects into a few jets is performed by applying a jet finding algorithm. The results presented in this paper are all obtained with the so-called inclusive, longitudinal invariant $k_\perp$ algorithm [1]. This algorithm has the advantage of being infrared and collinear safe and to be minimally sensitive to fragmentation and underlying event effects.

Reconstructed data are corrected from detector to hadron level using a full detector simulation. Next-to-leading order (NLO) QCD predictions are corrected from parton to hadron level. This involves the fragmentation of partons into hadrons and secondary interactions between partons of the photon and proton remnants. Correction factors are obtained from leading order (LO) Monte Carlo (MC) models where NLO effects are modelled by QCD cascades.

In LO two type of processes are distinguished. In direct processes the exchanged photon interacts as a whole with the proton to produce jets. In resolved interactions, the photon is treated as a source of partons, one of which produces a hard scattering with the proton, leaving a (soft) photon remnant behind. The concept of resolved photons is useful in photoproduction

[a] Postdoctoral fellow of the Fund for Scientific Research - Flanders (Belgium); Pierre.VanMechelen@ua.ac.be

as well as in deep-inelastic scattering (DIS) when $E_T^2 \gg Q^2$, where E_T is the transverse energy of the partons produced in the hard interaction and Q^2 is the virtuality of the exchanged photon. To separate direct and resolved enhanced event samples, the momentum fraction of the photon entering the hard scattering, x_γ, can be used. On hadron level, the variable x_γ^{jet}, which is correlated to the parton level x_γ, is calculated as $x_\gamma^{jet} = \sum_{jets} E_T^{jet} \mathrm{e}^{-\eta^{jet}}/2E_\gamma$ (with E_T^{jet} and η^{jet} the jet transverse energy and pseudorapidity and E_γ the exchanged photon energy).

Using QCD factorization, the direct and resolved cross sections for producing N jets, integrated over phase space, can be expressed as

$$\sigma_{direct}^{ep\to e+Njets+X} = \int_\Omega d\Omega f_{\gamma/e}(y,Q^2) \sum_i f_{i/p}(x_p,\mu_p^2)\sigma^{\gamma i\to Njets}, \quad (1)$$

$$\sigma_{resolved}^{ep\to e+Njets+X} = \int_\Omega d\Omega f_{\gamma/e}(y,Q^2) \sum_{ij} f_{i/p}(x_p,\mu_p^2) f_{j/\gamma}(x_\gamma,\mu_\gamma^2)\sigma^{ij\to Njets}. \quad (2)$$

Here $f_{\gamma/e}$, $f_{i/p}$ and $f_{j/\gamma}$ are flux factors for photons originating from the electron and for partons originating from the proton and the photon, respectively, evaluated at given fractional momentum-energies and factorization scales. The partonic cross sections $\sigma^{\gamma i\to Njets}$ and $\sigma^{ij\to Njets}$ can be calculated in LO or NLO as a function of the strong coupling constant $\alpha_S(\mu_R)$, where μ_R is the renormalization scale. The choice of renormalization and factorization scales will lead to some uncertainty in the predicted cross sections. Different NLO calculations further differ mainly in their treatment of infrared and collinear divergences.

2 Inclusive jet photoproduction

Figure 1 shows the first H1 data on inclusive jet photoproduction obtained with the $k_\perp$ algorithm[2]. This analysis comprises two data sets. At large E_T^{jet}, tracker and calorimeter information is emploid to trigger the data acquisition, while at low E_T^{jet} a trigger based on the presence of the scattered electron in an electron tagger is used, since in this kinematic range the first trigger suffers from large backgrounds. The low E_T^{jet} data points are corrected for the different Q^2 range covered, whereafter they agree well with the high E_T^{jet} data in the overlap region.

The cross section as function of E_T^{jet} is displayed in Fig. 1a. It falls over more than six orders of magnitude from $E_T^{jet} = 5$ to 75 GeV. LO QCD predictions underestimate the cross section (even with hadronisation corrections), especially at low E_T^{jet}, while NLO QCD models reproduce the data well after applying hadronisation corrections. Different choices of photon and proton PDF's vary at the level of 5 to 10 % and describe the data within errors.

Figure 1b shows the cross section as a function of η^{jet}, in two ranges of E_T^{jet}. It is observed that hadronisation corrections increase towards the proton remnant direction. For $E_T^{jet} >$ 12 GeV, the data are well described by NLO prediction, but at lower E_T^{jet} the data exhibit a faster rise towards the proton remnant direction than predicted by NLO QCD. This might be explained by a failure of the LO MC models to describe the hadronisation corrections properly, by the inadequacy of the photon PDF or by the need for higher order (HO) corrections.

The ZEUS Collaboration uses the measurement of jets in photoproduction to extract values for $\alpha_S(E_T^{jet})$ [3]. The jet cross section is fitted in each bin of E_T^{jet} to

$$[d\sigma/dE_T^{jet}]_i = A_i\alpha_S(E_T^{jet}) + B_i\alpha_S^2(E_T^{jet}), \quad (3)$$

where the constants A_i en B_i are obtained from NLO QCD calculations. A fit of the energy-scale dependence of the extracted $\alpha_S(E_T^{jet})$ to the renormalization group equation yields

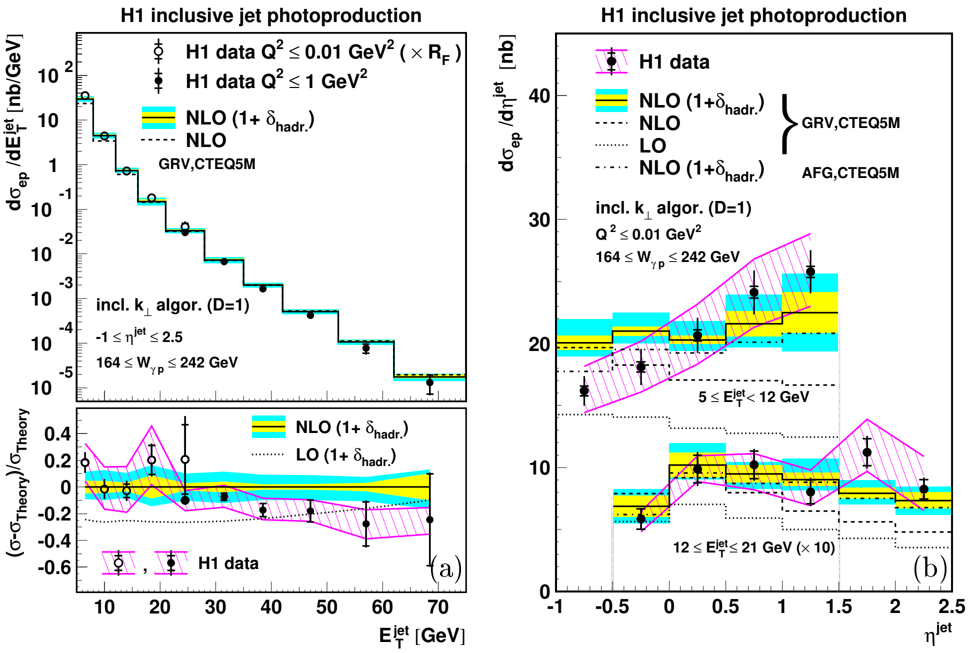

Figure 1: Differential inclusive jet cross sections as a function of E_T^{jet} (a) and η^{jet} (b). The hatched band shows the uncertainty associated with the LAr calorimeter energy scale. The inside and outside shaded bands represent the uncertainty from hadronisation corrections and from renormalization and factorization scales, respectively.

$$\alpha_S(M_Z) = 0.1224 \pm 0.0001(\text{stat.})^{+0.0022}_{-0.0019}(\text{syst.})^{+0.0054}_{-0.0042}(\text{theo.}). \tag{4}$$

This is in agreement with the current world average of 0.1183 ± 0.0027.

3 Dijet electroproduction

When the virtuality of the exchanged photon is much larger than the natural QCD mass scale ($Q^2 \gg \Lambda^2_{QCD}$), resolved photons are in principle not needed. However, LO QCD does not describe the data on dijet production and HO effects therefore need to be included.

The H1 Collaboration compares two approaches [4]. The first approach uses the HERWIG MC model [5] based on DGLAP QCD evolution with resolved photons. Both transversely and longitudinally polarized photons are needed to describe the measured cross section, as shown in Fig. 2. The second approach uses the CCFM evolution equations as implemented in the CASCADE MC model [6] with only direct photons. This model is equally well able to describe the data. It is therefore clear that the ordering of a single DGLAP cascade needs to be broken, but whether this can be achieved by introducing a second cascade originating from the photon or whether new QCD dynamics is needed can not be decided.

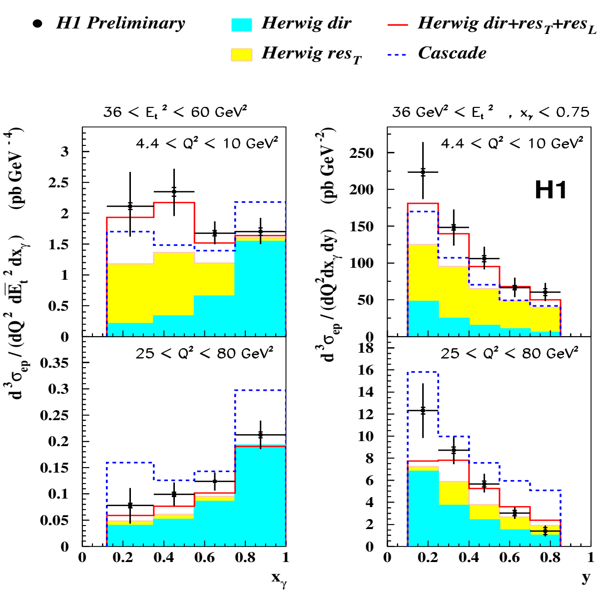

Figure 2: Differential cross section for dijet production as a function of x_γ or y in bins of Q^2 and average E_T^{jet}.

ZEUS computes the ratio of resolved to direct enhanced components of the dijet cross section [7] defined as:

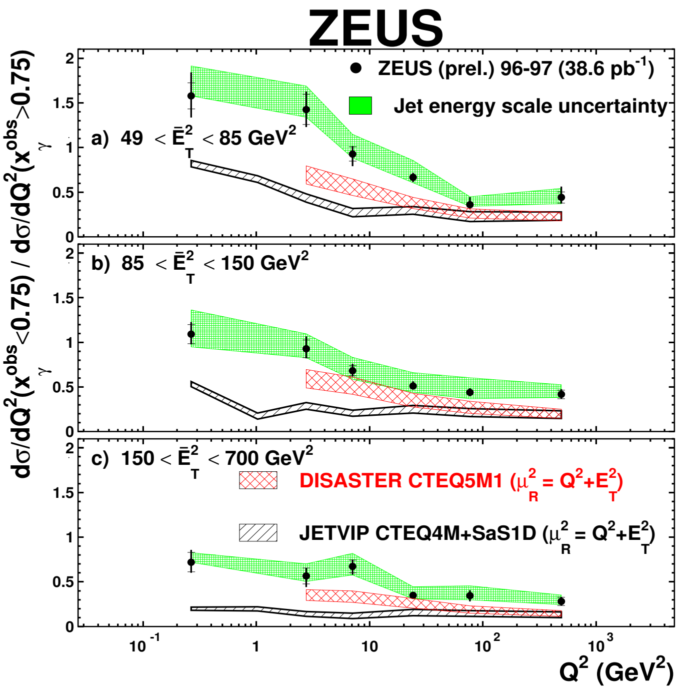

Figure 3: The ratio of resolved to direct enhanced components of the dijet cross section as function of Q^2 in bins of average E_T^{jet}.

$$R = \frac{\frac{d\sigma}{dQ^2}(x_\gamma^{jet} < 0.75)}{\frac{d\sigma}{dQ^2}(x_\gamma^{jet} > 0.75)}. \qquad (5)$$

Figure 3 shows R as a function of Q^2 in bins of average E_T^{jet}. Two NLO QCD models are used for comparisons. DISASTER++ [8] only incorporates pointlike photons, while JETVIP [9] implements both direct and resolved photons. Neither describes the ratio of resolved to direct enhanced components well and although JETVIP should produce a resolved enhanced component it actually performs worse than DISASTER++. ZEUS also observes, however, that the direct enhanced component by itself is well reproduced by both models.

4 Inclusive jet electroproduction

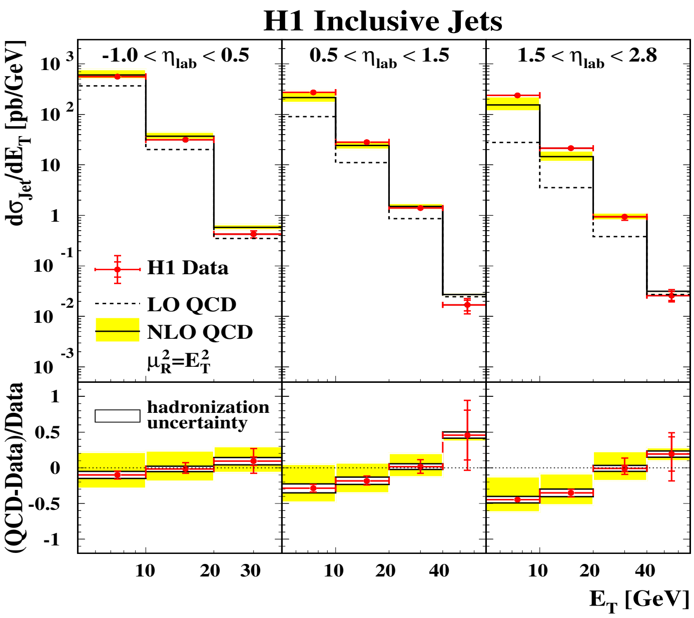

Figure 4: The inclusive jet cross section integrated over $5 < Q^2 < 100$ GeV^2 and $0.2 < y < 0.6$. The hatched band around the NLO prediction represents the renormalization scale uncertainty.

Inclusive jet cross sections obtained by H1 [10] are shown in Fig. 4. In the backward region and at all η_{lab}^{jet} for $E_T^{jet} > 20$ GeV, NLO QCD calculations by DISENT [11] describe the $d\sigma^{jet}/dE_T^{jet}$ distributions well. Deviations are, however, visible towards the proton remnant if both E_T^{jet} and Q^2 are small. These discrepancies are accompanied by large corrections between LO and NLO predictions.

Using a similar method as mentioned before, ZEUS has extracted values for $\alpha_S(E_T^{jet})$ [12]. The result is shown in Fig. 5 and is compared to the scale dependence from the renormalization group equation using as input value the result obtained from a fit to the measured $d\sigma^{jet}/dQ^2$ distribution for $Q^2 > 500$ GeV^2:

$$\alpha_S(M_Z) = 0.1212 \pm 0.0017(\text{stat.})^{+0.0023}_{-0.0031}(\text{syst.})^{+0.0028}_{-0.0027}(\text{theo.}). \qquad (6)$$

5 Conclusion

The H1 and ZEUS Collaborations have measured jet production in *ep* collisions with real and virtual photons in a large kinematic range. Cross sections are obtained with high accuracy and fall over more than six orders of magnitude as a function of transverse energy.

Competitive values for the strong coupling constant α_S are obtained which are in agreement with the current world average.

NLO QCD calculations do a very good job in describing jet cross section, with exceptions for forward jets at low Q^2 and E_T^{jet} and for the ratio of direct to resolved enhanced components in dijet production.

This wealth of new high-precision data can, and should, be used in global fits of photon and PDF's.

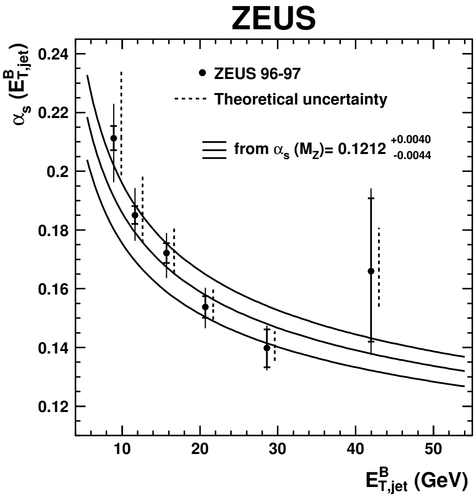

Figure 5: The $\alpha_S(E_T^{jet})$ values as determined from a QCD fit of the measured jet cross section.

Acknowledgments

I am indebted to all members of the H1 and ZEUS Collaborations who contributed to these results by collecting and analysing the experimental data.

References

1. S. D. Ellis and D. E. Soper, *Phys. Rev.* D **48**, 3160 (1993) [hep-ph/9305266].
2. H1 Collaboration, C. Adloff *et al.*, accepted by *Eur. Phys. J.* C [hep-ex/0302034].
3. ZEUS Collaboration, S. Chekanov *et al.*, accepted by *Phys. Lett. B* [hep-ex/0212064].
4. *Measurement of dijet cross sections at low Q^2 at HERA*, H1 Collaboration, conference paper submitted to the 31st International Conference on High Energy Physics, ICHEP02, July 24, 2002, Amsterdam.
5. G. Marchesini *et al.*, *Comput. Phys. Commun.* **67**, 465 (1992).
6. H. Jung, *Comput. Phys. Commun.* **86**, 147 (1995); H. Jung and G. P. Salam, *Eur. Phys. J.* C **19**, 351 (2001) [hep-ph/0012143].
7. *Virtual photon structure in dijet production at HERA*, ZEUS Collaboration, conference paper submitted to the 31st International Conference on High Energy Physics, ICHEP02, July 24, 2002, Amsterdam.
8. D. Graudenz [hep-ph/9710244].
9. B. Pötter, *Comput. Phys. Commun.* **133**, 105 (1997).
10. H1 Collaboration, C. Adloff *et al.*, *Phys. Lett.* B **542**, 193 (2002) [hep-ex/0206029].
11. S. Catani and M. H. Seymour, *Nucl. Phys.* B **485**, 291 (1997); erratum *Nucl. Phys.* B **510**, 503 (1997) [hep-ph/9605323].
12. ZEUS Collaboration, S. Chekanov *et al.*, *Phys. Lett.* B **547**, 164 (2002) [hep-ex/0208037].